



Alterations in Cognition-Related Cerebello-Cerebral Networks in Multiple System Atrophy

Kazuya Kawabata¹ · Kazuhiro Hara¹ · Hirohisa Watanabe² · Epifanio Bagarinao² · Aya Ogura¹ · Michihito Masuda¹ · Takamasa Yokoi¹ · Toshiyasu Kato¹ · Reiko Ohdake² · Mizuki Ito¹ · Masahisa Katsuno¹ · Gen Sobue^{2,3}

Published online: 8 May 2019

© Springer Science+Business Media, LLC, part of Springer Nature 2019

Abstract

We aimed to elucidate the effect of cerebellar degeneration in relation to cognition in multiple system atrophy (MSA). Thirty-two patients diagnosed with probable MSA and 32 age- and gender-matched healthy controls (HCs) were enrolled. We conducted voxel-based morphometry (VBM) for anatomical images and independent component analysis (ICA), dual-regression analysis, and seed-based analysis for functional images with voxel-wise gray matter correction. In the MSA group, a widespread cerebellar volume loss was observed. ICA and dual-regression analysis showed lower functional connectivity (FC) in the left executive control and salience networks in regions located in the cerebellum. Seed-based analysis using the identified cerebellar regions as seeds showed extensive disruptions in cerebello-cerebral networks. Global cognitive scores correlated with the FC values between the right lobules VI/crus I and the medial prefrontal/anterior cingulate cortices and between the same region and the amygdala/parahippocampal gyrus. Our study indicates that cerebellar degeneration in MSA causes segregation of cerebellar-cerebral networks. Furthermore, the cognitive deficits in MSA may be driven by decreased cerebello-prefrontal and cerebello-amygdaloid functional connections.

Keywords Multiple system atrophy · Cerebellum · Cognition · Functional connectivity · Resting-state network

Introduction

Multiple system atrophy (MSA) is a sporadic neurodegenerative disease characterized by varying degrees of cerebellar ataxia, parkinsonism, and autonomic failure. Although dementia based on the Diagnostic and Statistical Manual of

Mental Disorders (DSM)-IV is one of the nonsupporting features of MSA diagnosis [1], patients with MSA often manifest cognitive deficits during the course of the disease [2, 3]. Several studies demonstrated cognitive deficits in executive functions [4–6] and multiple domains including memory, language, and visuospatial abilities in MSA [7, 8]. Previous voxel-based morphometric studies using magnetic resonance imaging (MRI) showed that the frontal-temporal cortical and subcortical atrophic changes relate to not only executive dysfunction but also multiple cognitive deficits [9, 10], and memory scores correlate with prefrontal lobe atrophy [11]. Single-photon emission computed tomography (SPECT) [7] and fluorodeoxyglucose positron-emission tomography (FDG-PET) [12] have also revealed that cognitive deficits in MSA involve frontal dysfunction. In comparison, recent studies have demonstrated that involvement of subcortical pathways, such as the fronto-striatal pathway and corpus callosum, could be predominantly related to cognitive impairment in MSA [13, 14].

The cerebellum, which is highly involved in MSA, plays crucial roles in cognitive and emotional regulation [15–17]. Cerebellar lesions may lead to cerebellar cognitive affective

Kazuya Kawabata and Kazuhiro Hara contributed equally to this work.

Electronic supplementary material The online version of this article (<https://doi.org/10.1007/s12311-019-01031-7>) contains supplementary material, which is available to authorized users.

✉ Hirohisa Watanabe
nabe@med.nagoya-u.ac.jp

✉ Gen Sobue
sobueg@med.nagoya-u.ac.jp

¹ Department of Neurology, Nagoya University Graduate School of Medicine, Nagoya, Japan

² Brain and Mind Research Center, Nagoya University, Nagoya, Japan

³ Research Division of Dementia and Neurodegenerative Disease, Nagoya University Graduate School of Medicine, Nagoya, Japan

syndrome, which includes deficits in executive function, visual spatial processing, linguistic skills, and regulation of affect [15, 17]. Neuroimaging studies have demonstrated the cerebellar topography of cognitive functions in the posterior cerebellar lobe [18]. A recent study showed that the cerebellar cortex could be divided into several areas related to nonmotor function such as language, working memory, social cognition, and emotional experience using task-based fMRI images [19]. The divergent cerebello-basal ganglia-thalamo-cortical circuits can play an essential role in motor and nonmotor functions including cognition based on the proposed concept of the universal cerebellar transform [20, 21]. However, demonstrating the contribution of the polysynaptic circuit dysfunction to cognition using conventional MRI and diffusion tractography is still challenging. On the other hand, resting-state functional MRI (fMRI) may be applicable for such an analysis because resting-state networks (RSNs) generally reflect underlying polysynaptic anatomical pathways [22]. However, the relationship between cerebellum-related functional connectivity (FC) alterations and cognitive deficits in MSA remains unclear.

In this study, we hypothesized that cerebellar degeneration influences the cerebello-cerebral FC related to the cognitive functions observed in MSA. To clarify this hypothesis, we investigated large-scale RSNs related to the cerebellum extracted with independent component analysis (ICA) to find the voxel-level cerebellar alterations within the RSNs in MSA. The cerebellum has distinct regional contributions to the corresponding RSNs [23]. ICA is a data-driven approach and it enables us to extract the functionally different cerebellar subregions as nodes of RSNs without a priori hypothesis. Next, using cerebellar regions exhibiting aberrant connectivity as seeds, we also performed seed-based connectivity analysis to identify altered connections of the cerebello-cerebral networks especially related to cognition. The combination of ICA and seed-based analysis leads to clarify both within large-scale RSNs and seed-to-whole-brain connectivity alterations in MSA. In the analysis, we included voxel-wise gray matter (GM) values as covariates of no interest to minimize the effects of regional atrophies [24].

Materials and Methods

Participants

We enrolled 32 patients diagnosed with probable MSA according to the second consensus criteria by expert neurologists [1]: 29 patients from our previous tract-based spatial statistics (TBSS) study [14] and 3 newly recruited patients. One patient who participated in the study was excluded because of excessive head motion during scans. Thirty-two age- and gender-matched healthy controls (HC) were also

incorporated from our ongoing healthy aging cohort study at Brain and Mind Research Center, Nagoya University, Japan [25]. Written informed consent was obtained from all participants. The study conformed to the Ethical Guidelines for Medical and Health Research Involving Human Subjects endorsed by the Japanese government and was approved by the Ethics Committee of Nagoya University Graduate School of Medicine.

Clinical Assessments

Patients with MSA underwent the Mini-Mental State Examination (MMSE), the Japanese version of Addenbrooke's Cognitive Examination-Revised (ACE-R) [26, 27], and the unified MSA rating scales (UMSARS) part I, II, and IV [28]. ACE-R can be readily adopted in approximately 15 min and can provide a more comprehensive assessment of a general cognitive function than the MMSE or the Montreal Cognitive Assessment (MoCA). ACE-R includes subdomain scores for evaluating the frontal lobe function such as attention and fluency, which are frequently involved in MSA. In addition, recent meta-analysis studies have shown that ACE-R is one of the best screening batteries for detecting dementia [29] and is also useful for evaluating cognition in other neurodegenerative diseases [30].

MRI Acquisition

MRI scans were performed using a Siemens Magnetom Verio (Siemens, Erlangen, Germany) 3.0-T scanner with a 32-channel head coil at the Brain and Mind Research Center of Nagoya University. High-resolution T1-weighted images (T1-WI) were acquired using the following parameters: repetition time (TR) = 2.5 s, echo time (TE) = 2.48 ms, 192 sagittal slices with a distance factor of 50% and 1-mm thickness, field of view (FOV) = 256 mm, 256 × 256 matrix size, and an in-plane voxel resolution of 1 × 1 mm². Resting-state functional images were obtained with echo-planar imaging (EPI) using the following parameters: TR = 2.5 s, TE = 30 ms, 39 transversal slices with a 0.5-mm interslice interval and 3-mm thickness, FOV = 192 mm, 64 × 64 matrix dimension, flip angle = 80°, and 198 volumes. The participants were instructed to stay awake and close their eyes during the 8-min scan.

Voxel-Based Morphometry Analysis

T1-WI were preprocessed by the following processes using Statistical Parametric Mapping 12 software (SPM12; Wellcome Trust Center for Neuroimaging, London, UK; <http://www.fil.ion.ucl.ac.uk/spm/software/spm12/>) running on MATLAB (R2016a; MathWorks, Natick, MA, USA): anatomical images were (i) segmented into component images including GM, white matter

(WM), cerebrospinal fluid (CSF), and nonbrain tissues, (ii) normalized to the standard Montreal Neurological Institute (MNI) space using Diffeomorphic Anatomical Registration using Exponentiated Lie algebra (DARTEL) [31], (iii) resampled to an isotropic voxel resolution of $2 \times 2 \times 2 \text{ mm}^3$, and (iv) smoothed using an 8-mm full-width-at-half-maximum (FWHM), isotropic Gaussian filter. The total intracranial volume (TIV) was estimated as the sum of GM, WM, and CSF. We performed a two-sample *t*-test to compare the MSA and HC groups and conducted multiple regression analysis only in the MSA group, including the ACE-R scores as covariates of interest. Age, gender, and TIV were included as covariates of no interest in the analysis. The obtained statistical maps were generated at corrected $p < 0.05$ for multiple comparisons using a cluster-level family-wise error rate (FWE) with the cluster-forming threshold set at $p = 0.001$. Extracted GM values were adjusted for age, gender, and TIV using a general linear model. Anatomical location was estimated using xjView toolbox (<http://www.alivelearn.net/xjview8>). Preprocessed anatomical images were also used as covariates in the functional imaging analysis.

Resting-State fMRI Analysis

Preprocessing

Functional images were also preprocessed using SPM12. Briefly, the first 5 volumes were discarded to remove the initial image inhomogeneity. Then, the functional images were (i) slice time corrected relative to the middle slice, (ii) realigned relative to the mean functional image, (iii) coregistered to the bias-corrected T1-WI, (iv) normalized to the MNI space using the transformation information obtained during segmentation, (v) resampled to an isotropic voxel resolution of $2 \times 2 \times 2 \text{ mm}^3$, and (vi) spatially smoothed using an 8-mm FWHM Gaussian filter. Additionally, we regressed out 24 motion-related regressors [$R_t R_t^2 R_{t-1} R_{t-1}^2$], where $R = [x, y, z, \text{roll}, \text{pitch}, \text{yaw}]$ represents the estimated motion parameters (3 translations and 3 rotations) for motion correction. Using motion parameters, we also calculated framewise displacement (FD) [32]. Signals extracted from spherical regions-of-interest (ROIs) within the CSF (center = [20, -32, 18], radius = 4 mm) and WM (center = [24, -12, 34], radius = 4 mm), the global signal, and the signals' derivatives were also removed. Finally, the preprocessed data were then bandpass filtered within 0.01–0.1 Hz. The additional preprocessing was performed using in-house MATLAB scripts. The resulting dataset was used in the subsequent analysis. We did not incorporate the participants with excessive head motion of mean FD value over 0.5 through EPI scans in the analysis.

Group ICA and Dual-Regression Analysis

To analyze the preprocessed functional images, we used ICA as implemented in the MELODIC, component software of the FSL package [33]. All participants' images were temporally concatenated and decomposed into 20 independent components (IC) spatial maps to examine large-scale cerebello-cerebral RSNs [34]. We visually identified eight RSNs with some nodes located in the cerebellum: the dorsal default mode network (DMN), the left executive control network (ECN), the right ECN, the language network, the ventral DMN, the salience network (SN), the sensorimotor network, and the cerebellum network (Fig. 1). Cerebellar locations of each network were consistent with those in previous healthy participant studies [23]. We tested the intergroup differences in RSNs using dual-regression analysis and randomize, a nonparametric approach, with 5000 permutations for each component of interest [35]. We included age, gender, and voxel-wise GM values from the preprocessed anatomical images as covariates of no interest [24]. Reported statistical maps were FWE-corrected for multiple comparisons with threshold-free cluster enhancement (TFCE). We extracted mean regional functional connectivity (MRFC) from cerebellar regions exhibiting significantly decreased FC and created ROIs from these regions for the subsequent seed-based analysis.

Seed-Based Analysis

To generate connectivity maps, time series within each ROI were extracted from the preprocessed resting-state data. For each ROI, the resulting mean time series was correlated with the time series from all voxels within the brain. The computed correlation coefficients were converted into *z*-scores using the Fisher transform. Using the generated connectivity maps, two-sample *t*-tests were performed to examine intergroup differences between the MSA and HC groups. Multiple regression analyses were also conducted only among patients with MSA to identify regions with connectivity values from the seed that correlated with the ACE-R scores. Age, gender, and voxel-wise GM value were included as covariates of no interest. To conduct the analysis with voxel-wise GM correction, we used VoxelStats toolbox [36]. Statistical significance was set at $p < 0.05$, corrected for multiple comparisons using a cluster-level FWE with a cluster-forming threshold set at $p = 0.001$ based on random field theory. The resulting clusters were visualized using BrainNet Viewer [37], and the MRFC of the clusters was extracted from the connectivity maps.

Statistical Analysis

The intergroup differences of demographics and cognitive scores were tested using the χ -square test for gender and the Mann-Whitney *U* test for others. Spearman's rank correlation

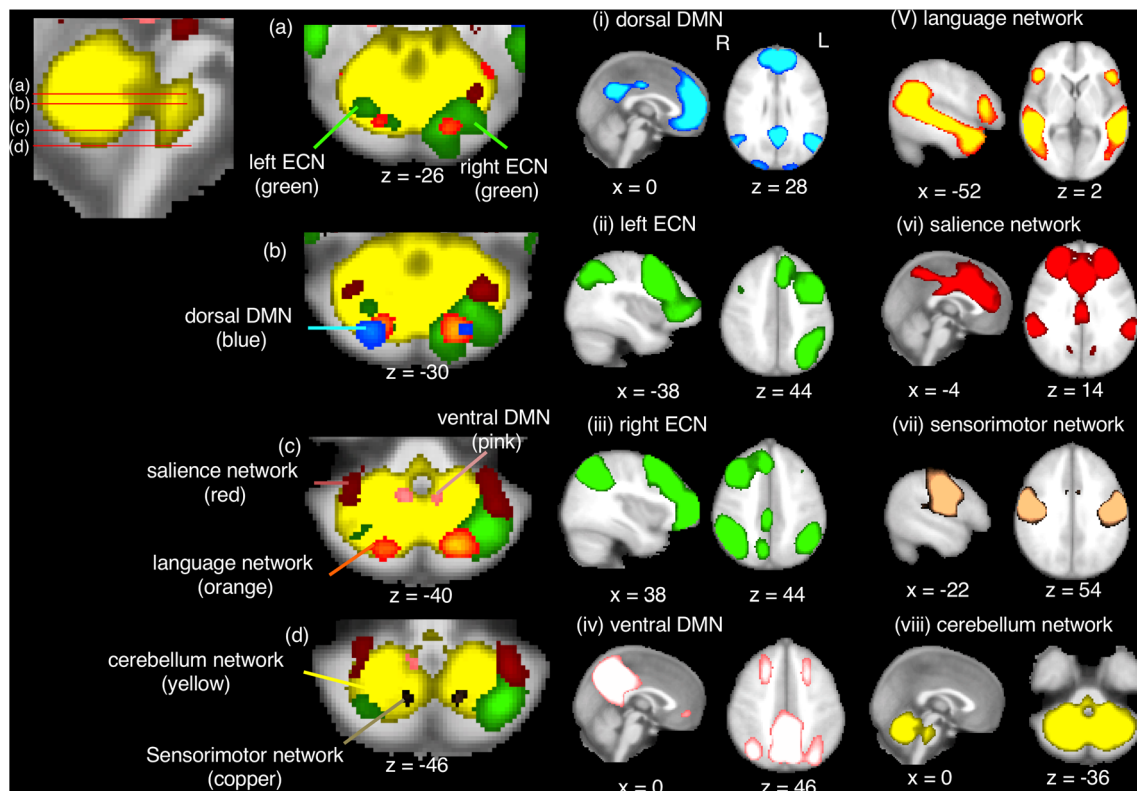


Fig. 1 Resting-state networks related to the cerebellum. Eight RSNs: (i) dorsal DMN (blue–light blue), (ii) left ECN (green), (iii) right ECN (green), (iv) ventral DMN (pink), (v) language network (red - yellow),

(vi) SN (red), (g) sensorimotor network (copper), (h) cerebellum-brainstem network (yellow). DMN, default-mode network; ECN, executive control network; RSNs, resting-state networks

test was performed to obtain the correlation coefficients between measured values or scores. Analyses were conducted with MATLAB and R version 3.3.2 (<http://www.r-project.org/>).

Results

Demographics

The demographics of the MSA group and the HC group are shown in Table 1. The MMSE scores and the ACE-R scores of the MSA group were significantly lower than those of HCs. FD values, which represent estimated head motion parameters, were not significantly different between the two groups. In the MSA group, 13 patients were taking levodopa, and none were taking acetylcholinesterase inhibitors.

VBM Analysis Results

Compared with the HC group, the MSA group exhibited significant GM volume reductions throughout the cerebellum ($p < 0.05$, cluster-level FWE-corrected for multiple comparisons, Fig. 2), but not in the cerebrum. In the MSA group,

multiple regression analysis did not reveal any regions in which volume significantly correlated with the ACE-R scores.

ICA and Dual-Regression Analysis Results

Dual-regression analysis revealed that the MSA group had significantly lower FC regions in the cerebellum in 2 out of 8 RSNs than the HC group: right lobules VI and crus I within the left ECN and left lobule VI within the SN ($p < 0.05$, corrected for multiple comparisons, Fig. 3a, b). In the MSA group, the MRFC of these regions did not correlate with the ACE-R scores (Spearman's rho = 0.23 and 0.16, $p = 0.21$ and 0.37, respectively).

Seed-Based Analysis: Cerebello-Cerebral FC in MSA

From both ROIs of the left ECN and SN, which were generated from identified cerebellar regions exhibiting aberrant FC (shown in Fig. 3a and b), lower FC regions were mainly found in the prefrontal, parietal, and cingulate cortices, basal ganglia, and thalamus in the MSA group (Fig. 4a and b, detailed coordinates and cluster size are shown in supplementary Table S1). A broad range of cortical regions showing decreased FC from the seed ROIs overlapped with the respective RSNs.

Table 1 Demographics of participants

	MSA (N = 32)	HC (N = 32)	<i>p</i> value
Demographics			
Age (year)	63.4 (7.8)	63.4 (7.6)	1.000 ¹
Gender (M/F, n)	18/14	18/14	1.000 ²
Clinical			
Diagnosis(C/P, n)	19/13	–	
Duration (year)	2.8 (1.5)	–	
UMSARS part 1	18.5 (7.4)	–	
UMSARS part 2	20.4 (8.6)	–	
UMSARS part 4	2.4 (0.9)	–	
Cognition			
MMSE	27.2 (2.5)	29.5 (0.7)	< 0.001 ¹
ACE-R total	86.2 (9.1)	96.1 (2.2)	< 0.001 ¹
ACE-R subdomain scores			
Attention/orientation	17.1 (1.2)	18.0 (0.2)	< 0.001 ¹
Memory	20.6 (4.5)	23.9 (1.6)	< 0.001 ¹
Verbal fluency	10.1 (3.0)	13.5 (1.0)	< 0.001 ¹
Language	24.0 (2.0)	25.0 (0.9)	0.037 ¹
Visuospatial ability	14.4 (1.9)	15.7 (0.6)	< 0.001 ¹
Image–head motion			
Mean FD	0.20 (0.10)	0.23 (0.11)	0.317 ¹

Data are expressed as mean (SD)

¹ Mann-Whitney *U* test

² Chi-square test

Seed-Based Analysis: Cerebello-Cerebral FC and Cognitive Performances in MSA

From the ROI of the left ECN, the FC of two clusters positively correlated with the ACE-R total scores. These clusters were located in the medial prefrontal and anterior cingulate cortices corresponding to Brodmann area 9 and 10 and in the

left medial temporal lobe, including amygdala and parahippocampal gyrus (Fig. 5). No significant regions were found for the ROI from the SN.

The correlation between the extracted MRFC of each cluster and the ACE-R total/subdomain scores is shown in Fig. 6 and Table 2. The cluster in the prefrontal cortex was more related to verbal fluency and memory scores ($\rho = 0.65$ and 0.47 , respectively), whereas the cluster in the medial temporal lobe was more related to language and visuospatial abilities ($\rho = 0.55$ and 0.51 , respectively).

Discussion

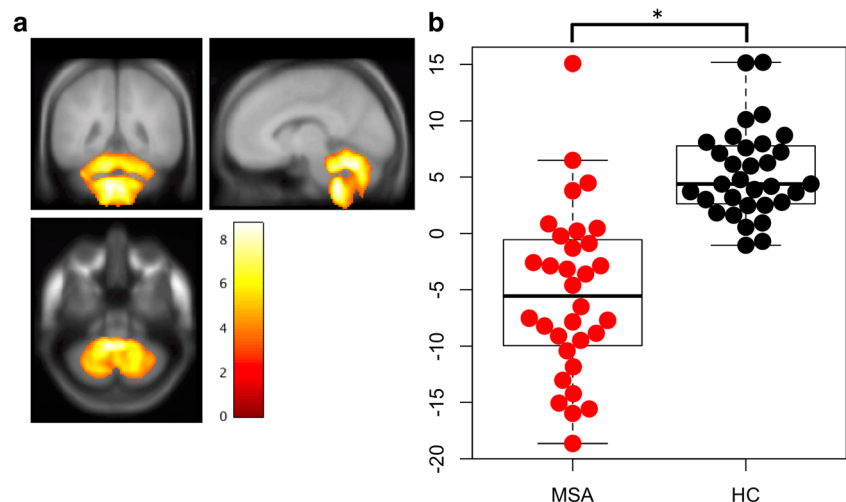
Findings

Our major findings are as follows: the MSA group showed (i) reductions in cerebellar FC within the left ECN and the SN among the RSNs related to the cerebellum, (ii) a broad range of regions with decreased FC in the cerebrum from these cerebellar seed regions with decreased FC compared with the HC group, (iii) the correlation between the general cognitive battery scores and FC between the seed region from the left ECN (right lobules VI/crus I) and the medial prefrontal/anterior cingulate cortices as well as the left amygdala/parahippocampal gyrus.

Aberrant RSNs in the Cerebellum in MSA

RSNs have their own behavioral function characteristics [38]; however, the functional influences of the cerebellum on RSNs are still elusive. In our study, the ECN and the SN, which relate to several cognitive processes [38], showed aberrant cerebellar FC in MSA. However, the

Fig. 2 Voxel-based morphometric results. **a** Significant GM volume reductions were observed in the MSA group ($p < 0.05$, cluster-level FWE-corrected for multiple comparisons; the regions are shown as red–yellow). **b** Regional GM volume in the cluster adjusted for age, gender, and TIV. $*p < 0.001$. FWE; family-wise error rate; GMV, gray matter value; MNI, Montreal Neurological Institute; TIV, total intracranial volume



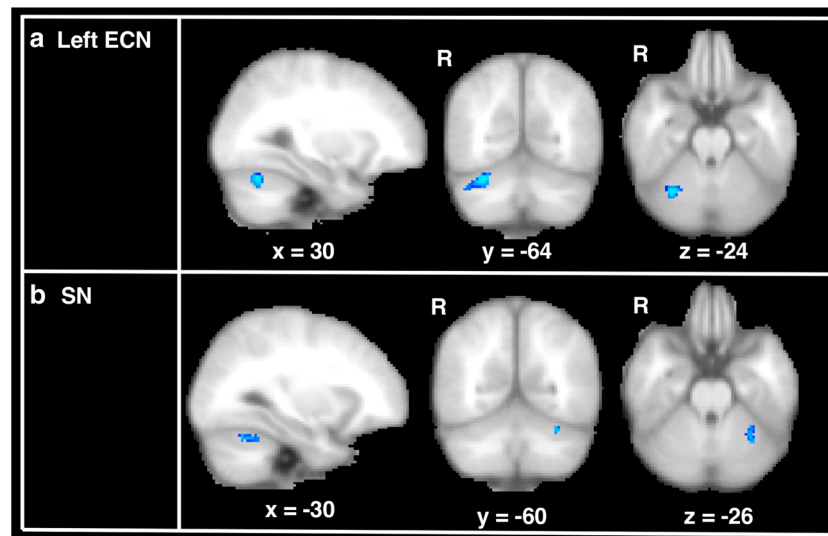


Fig. 3 Independent component analysis and dual-regression analysis results. Cerebellar regions with decreased FC in the cerebellum in the MSA group compared with those in the HC group ($p < 0.05$, FWE-corrected with TFCE). Blue–light blue indicates lower FC regions in the MSA group. **a** Cerebellar regions with decreased FC within the left ECN; peak MNI coordinates $(x, y, z) = (30, -64, -24)$, cluster size = 139.

b Cerebellar region with decreased FC within the SN; peak MNI coordinates $(x, y, z) = (-30, -60, -26)$, cluster size = 44. ECN, executive control network; FC, functional connectivity; HC, healthy control; MSA, multiple system atrophy; MNI, Montreal Neurological Institute; SN, salience network

strength of MRFC values within the regions with decreased FC did not correlate with the general cognitive scores; therefore, we performed seed-based analysis using aberrant FC regions in the cerebellum as seeds for detecting cerebello-cerebral FC in relation to cognition.

Disrupted Functional Cerebello-Cerebral Network

Seed-based analysis showed that, in the MSA group, regions from the ROI of the left ECN and that of the SN with lower FC were predominantly found in the frontal

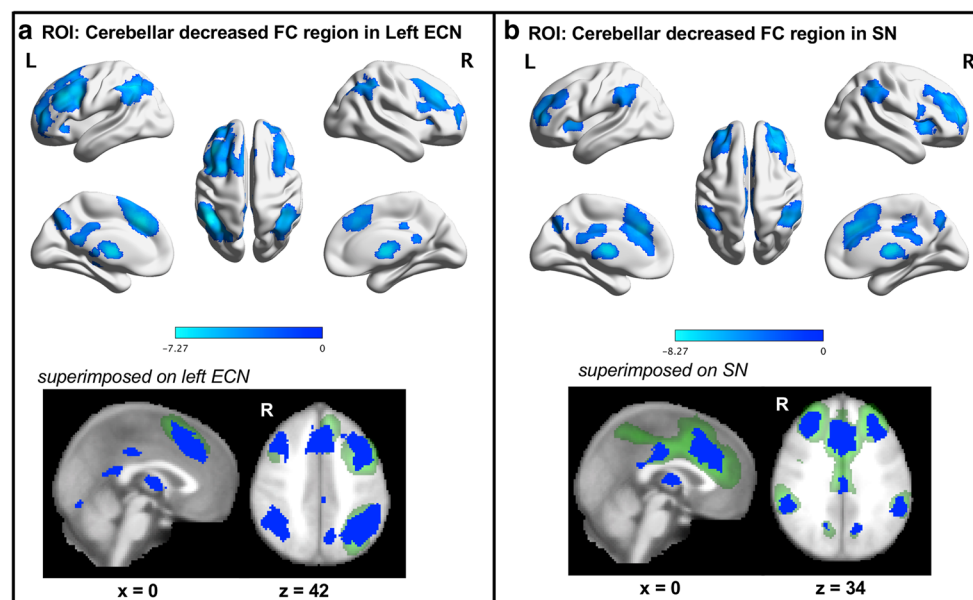
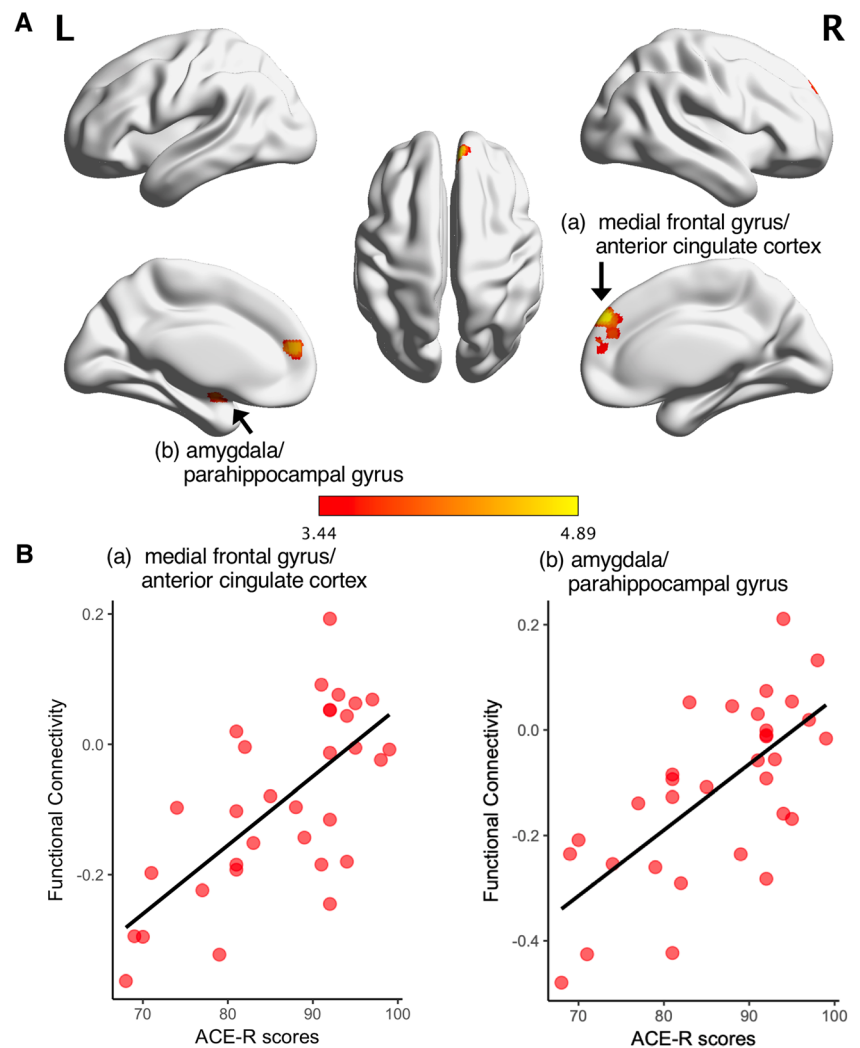


Fig. 4 Seed-based analysis results: region with decreased FC in the MSA group. **a** ROI, cerebellar regions with decreased FC in the left ECN (shown in Fig. 3a). **b** ROI, cerebellar regions with decreased FC in the SN (shown in Fig. 3b). The upper figures show regions with decreased FC from the seed ROI in the MSA compared with that in the HC group. Blue–light blue indicates regions with lower FC in the MSA group.

Lower figures show the regions with decreased FC superimposed on the corresponding RSN of the ROI. Detailed coordinates and cluster size are shown in supplementary Table 1. ECN, executive control network; FC, functional connectivity; HC, healthy control; ROI, region of interest; RSN, resting-state network; SN, salience network

Fig. 5 Seed-based analysis results: correlation with the ACE-R scores. **a** Red-yellow indicates the regions with FC positively correlated with the ACE-R scores from the ROI of the left ECN ($p < 0.05$, cluster-level FWE-corrected for multiple comparison). **(a)** Medial prefrontal cortex and anterior cingulate cortex; peak coordinates (x, y, z) = (4, 48, 36), cluster size = 227. **(b)** Amygdala and parahippocampal gyrus; peak coordinates (x, y, z) = (-22, 0, -12), cluster size = 92. **b** Scatter plot of individual MRFC and ACE-R scores from clusters shown in **a**. **(a)** Medial frontal gyrus and anterior cingulate cortex (Spearman's $\rho = 0.66$, $p < 0.001$). **(b)** Amygdala and parahippocampal gyrus (Spearman's $\rho = 0.63$, $p < 0.001$). ACE-R, Addenbrooke's Cognitive Examination-Revised; FC, functional connectivity; FWE, family-wise error; HC, healthy controls; ROI, region of interest; MRFC, mean regional functional connectivity



and parietal cortices mostly in regions related to the corresponding RSNs, basal ganglia, and thalamus. Posterior cerebellar lobules have anatomical and functional connections to the prefrontal and parietal lobes through subcortical structures such as the thalamus and basal ganglia [39–41]. Previous studies documented the cerebello-basal ganglia-thalamo-cortical functional disconnections relate to essential tremor [42], resting tremor in PD [43], and focal dystonia [44–46]. Yao et al. reported that cerebello-cortical dysfunction relates to the disease severity in MSA [47]. In our study, a broad range of regions with cerebello-cerebral FC disruption from ROIs was observed in the MSA group, especially the regions within the respective RSNs. We did not verify the relationship between the motor symptoms and cerebello-cerebral segregation in this study, but our results suggest that cerebellar degeneration in MSA causes an extensive disconnection of the cerebello-cerebral network.

Cerebello-Cerebral FC and Cognitive Performance

In our study, global cognitive performance correlated with FC between cerebellar lobules VI/crus I where we observed significant decreases in FC in the left ECN and prefrontal cortex and between lobules VI/crus I and the amygdala/parahippocampal gyrus. The area around the right cerebellar lobules VI and crus I is associated with language, working memory, and executive functions [48]. The medial prefrontal cortex, which is a part of the dorsal DMN, has many anatomical connections in the brain and plays a key role in executive function and memory [49, 50]. Task-based fMRI has shown that cognitive tasks, which relate to executive function or language, activate the posterior cerebellar lobules VI and VII as well as prefrontal and parietal cortices in healthy participants [51, 52] and that language function is right lateralized [48, 52]. These previous reports support our results that the FC between cerebellar lobules VI/crus I and prefrontal/cingulate cortices,

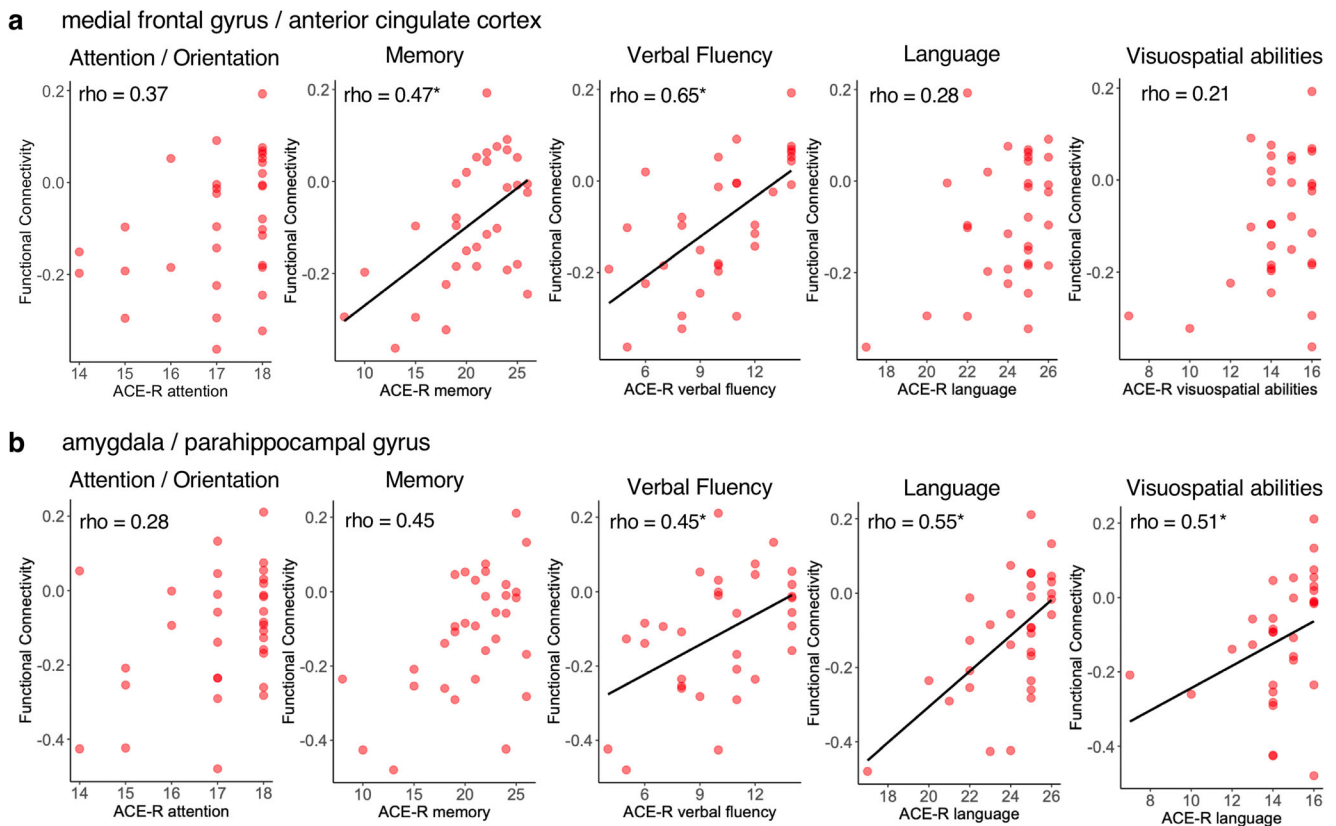


Fig. 6 Scatter plot of individual MRFC and ACE-R subscores. **a** MRFC between the medial frontal gyrus/anterior cingulate cortex and right cerebellar lobule VI/crus I. **(b)** MRFC between amygdala/parahippocampal gyrus and right cerebellar lobule VI/crus I. Each rho

and p values were shown in Table 2. *Indicates corrected $p < 0.05$ for multiple comparisons using Bonferroni correction. ACE-R, Addenbrooke's Cognitive Examination-Revised; MRFC, mean regional functional connectivity

which is associated with the dorsal DMN, may play a key role in cognitive deficits in patients with MSA.

On the other hand, the cognition-related functional connections between the right posterior cerebellum and the left amygdala/parahippocampal gyrus have been poorly understood, although recent studies have reported limbic cerebello-amygdaloid networks using ICA [53]. Interestingly, FC between posterior cerebellar lobules and limbic amygdala/parahippocampal gyrus was more related to the language and visuospatial ability subdomain scores than those of memory and verbal fluency. The amygdala has extensive connections to cortical and subcortical structures and relates to various functions of emotion, behavior, and cognition [54], while the parahippocampal gyrus is associated with several cognitive processes, including visuospatial, contextual association processing, and episodic memory [55]. Pathologically, the mesial temporal lobe, including the amygdala/parahippocampal gyrus, as well as the prefrontal cortex, where FC from the cerebellum was related to cognition in our study, tends to be involved in neuronal inclusions even at early stages in MSA [56]. Pathological substrates could influence brain network architecture in neurodegenerative disorders [57]. Although our findings are not necessarily indicative of

a pathological burden, subtle vulnerability may drive interregional FC aberration. Further studies are needed to shed light on the cognition-related network alterations in relation to pathological progression.

Divergent cerebellar roles have recently attracted more attention in line with the universal cerebellar transform theory [17, 21]. The cerebellum is associated with several nonmotor functions including not only cognition and emotion but also prediction of sequences [58] and motor timing [59–62], among others. The dysmetria of thought theory has been proposed as the mechanism of cognitive deficits derived from cerebellar dysfunction [17, 21]. Sokolov et al. documented the generalized concept of prediction and error-based learning from sensorimotor forward model for understanding cerebellar cognitive function [63]. In spite of the growing evidence of cerebellar nonmotor functions and cerebellar circuitry, these mechanisms have not been fully understood yet [64]. Our study may provide new insights into the functional architecture in the brain of the cognitive deficits in MSA in relation to the cerebello-cortical network contributions.

Recently, a large multicenter cohort study showed that a cognitively impaired MSA group exhibited only focal atrophy compared with cognitively normal MSA group [13]. The

Table 2 Correlation between MRFC and ACE-R total/subdomain scores

	Medial prefrontal cortex		Amygdala/parahippocampal gyrus	
	Rho	<i>p</i> value	Rho	<i>p</i> value
ACE-R total score	0.66	< 0.001	0.63	< 0.001
Subdomain scores				
Attention/orientation	0.37	0.038	0.28	0.115
Memory	0.47	0.006*	0.45	0.010
Verbal fluency	0.65	< 0.001*	0.45	0.009*
Language	0.28	0.119	0.55	0.001*
Visuospatial abilities	0.21	0.248	0.51	0.003*

*Corrected $p < 0.05$, using Bonferroni correction

authors conjectured that the contributions of cortical pathology to cognitive impairment in MSA were only marginal and proposed that the cognitive impairment is driven by focal fronto-striatal alterations based on subcortical degeneration. Franciotti et al. reported DMN abnormalities prior to cortical thickness changes in MSA [65]. We recently reported that anterior corpus callosal involvement was related to cognitive deficits [14]. In this study, we did not find that cortical atrophy was associated with cognition, but disconnection of cerebello-prefrontal and cerebello-amygdaloid/parahippocampal FC in relation to the cognitive impairment was prominent. These results suggest that cognitive deficits in MSA may be caused by subcortical network dysfunction antecedent to the cortical atrophic contribution.

Anatomical Change and FC in MSA

In the MSA group, VBM analysis showed extensive volume reductions in the cerebellum, but not in the basal ganglia or cortices. These results may reflect the features of MSA in East Asia, which is predominantly of the cerebellar type with a tendency toward cerebellar atrophic changes even in a majority of those with parkinsonian subtype (MSA-P) [66, 67]. To take into account the effect of this regional atrophy, we performed functional imaging analysis with GM correction [24]. Damoiseaux et al. reported smaller changes in cluster size with GM correction than without [68]. Regional atrophy could drive FC toward either an increase or decrease [69]. We believe that considering the effect of local atrophy when analyzing the neurodegenerative disorders that manifest specific anatomical changes is important.

Limitations

There were several limitations in this study. First, cerebellar atrophy was prominent in our population as discussed above. Second, our results could not provide information about causality of the network alteration; therefore, the cerebello-cerebral networks may be affected by focal cortical or

subcortical degeneration as well as cerebellar dysfunction, even though VBM analysis did not show cortical atrophic changes in the MSA group. In other words, network alterations may be affected by a third-party region. Third, although ACE-R is a brief and comprehensive battery, examining the effect of each cognitive domain requires more domain-specific cognitive batteries. Fourth, although dopamine replacement therapy is less effective in MSA than in PD, the medication can affect the functional topology in the brain. Lastly, this is a cross-sectional study; hence, future longitudinal studies are needed to clarify the FC changes in relation to MSA disease progression.

Conclusions

In the MSA group, cerebellar degeneration leads to alterations in cerebellar-related RSNs and causes cerebello-cerebral disconnection. In addition, the segregation of the cerebello-prefrontal and cerebello-amygdaloid/parahippocampal networks may be related to cognitive deficits in MSA.

Funding Information This study was partially supported by a Grant-in-Aid from the Research Committee of Central Nervous System Degenerative Diseases by the Ministry of Health, Labour, and Welfare, Integrated Research on Neuropsychiatric Disorders project carried out Strategic Research Program for Brain Sciences (SRPBS), a Grant-in-Aid for Scientific Research on Innovative Areas (Brain Protein Aging and Dementia Control 26117002) from the Ministry of Education, Culture, Sports, Science, and Technology of Japan, and Integrated Research on neuropsychiatric disorders carried out under the SRPBS, Scientific Research on Innovative Areas (Comprehensive Brain Science Network), and Integrated Research on Depression, Dementia and Development Disorders by SRPBS from Japan Agency for Medical Research and Development.

Compliance with Ethical Standards

This study conformed to the Ethical Guidelines for Medical and Health Research Involving Human Subjects endorsed by the Japanese government and was approved by the Ethics Committee of Nagoya University Graduate School of Medicine.

Conflict of Interest The authors declare that they have no conflict of interest.

References

- Gilman S, Wenning GK, Low PA, Brooks DJ, Mathias CJ, Trojanowski JQ, et al. Second consensus statement on the diagnosis of multiple system atrophy. *Neurology*. 2008;71(9):670–6.
- Stankovic I, Krismer F, Jesic A, Antonini A, Benke T, Brown RG, et al. Cognitive impairment in multiple system atrophy: a position statement by the neuropsychology task force of the MDS multiple system atrophy (MODIMSA) study group. *Mov Disord*. 2014;29(7):857–67.
- Asi YT, Ling H, Ahmed Z, Lees AJ, Revesz T, Holton JL. Neuropathological features of multiple system atrophy with cognitive impairment. *Mov Disord*. 2014;29:884–8.
- Kao AW, Racine CA, Quitania LC, Kramer JH, Christine CW, Miller BL. Cognitive and neuropsychiatric profile of the synucleinopathies: Parkinson disease, dementia with Lewy bodies, and multiple system atrophy. *Alzheimer Dis Assoc Disord*. 2009;23:365–70.
- Brown RG, Lacomblez L, Landwehrmeyer BG, Bak T, Utner I, Dubois B, et al. Cognitive impairment in patients with multiple system atrophy and progressive supranuclear palsy. *Brain*. 2010;133:2382–93.
- Siri C, Duerr S, Canesi M, Delazer M, Esselink R, Bloem BR, et al. A cross-sectional multicenter study of cognitive and behavioural features in multiple system atrophy patients of the parkinsonian and cerebellar type. *J Neural Transm (Vienna)*. 2013;120:613–8.
- Kawai Y, Suenaga M, Takeda A, Ito M, Watanabe H, Tanaka F, et al. Cognitive impairments in multiple system atrophy: MSA-C vs MSA-P. *Neurology*. 2008;70(16 Pt 2):1390–6.
- Auzou N, Dujardin K, Biundo R, Foubert-Samier A, Barth C, Duval F, et al. Diagnosing dementia in multiple system atrophy by applying Movement Disorder Society diagnostic criteria for Parkinson's disease dementia. *Parkinsonism Relat Disord*. 2015;21:1273–7.
- Kim JS, Yang JJ, Lee DK, Lee JM, Youn J, Cho JW. Cognitive impairment and its structural correlates in the parkinsonian subtype of multiple system atrophy. *Neurodegener Dis*. 2015;15:294–300.
- Lee MJ, Shin JH, Seoung JK, Lee JH, Yoon U, Oh JH, et al. Cognitive impairments associated with morphological changes in cortical and subcortical structures in multiple system atrophy of the cerebellar type. *Eur J Neurol*. 2016;23:92–100.
- Chang CC, Chang YY, Chang WN, Lee YC, Wang YL, Lui CC, et al. Cognitive deficits in multiple system atrophy correlate with frontal atrophy and disease duration. *Eur J Neurol*. 2009;16(10):1144–50.
- Lyoo CH, Jeong Y, Ryu YH, Lee SY, Song TJ, Lee JH, et al. Effects of disease duration on the clinical features and brain glucose metabolism in patients with mixed type multiple system atrophy. *Brain*. 2008;131(Pt 2):438–46.
- Fiorenzato E, Weis L, Seppi K, et al. Brain structural profile of multiple system atrophy patients with cognitive impairment. *J Neural Transm (Vienna)*. 2017;124(3):293–302.
- Hara K, Watanabe H, Bagarinao E, Kawabata K, Yoneyama N, Ohdake R, et al. Corpus callosal involvement is correlated with cognitive impairment in multiple system atrophy. *J Neurol*. 2018;265(9):2079–87.
- Schmahmann JD, Sherman JC. The cerebellar cognitive affective syndrome. *Brain*. 1998;121(Pt 4):561–79.
- Buckner RL. The cerebellum and cognitive function: 25 years of insight from anatomy and neuroimaging. *Neuron*. 2013;80(3):807–15.
- Schmahmann JD. The cerebellum and cognition. *Neurosci Lett*. 2019;688:62–75.
- Koziol LF, Budding D, Andreasen N, D'Arrigo S, Bulgheroni S, Imamizu H, et al. Consensus paper: the cerebellum's role in movement and cognition. *Cerebellum*. 2014;13(1):151–77.
- Guell X, Gabrieli JDE, Schmahmann JD. Triple representation of language, working memory, social and emotion processing in the cerebellum: convergent evidence from task and seed-based resting-state fMRI analyses in a single large cohort. *Neuroimage*. 2018;172:437–49.
- Caligiore D, Pezzulo G, Baldassarre G, Bostan AC, Strick PL, Doya K, et al. Consensus paper: towards a systems-level view of cerebellar function: the interplay between cerebellum, basal ganglia, and cortex. *Cerebellum*. 2017;16:203–29.
- Guell X, Gabrieli JDE, Schmahmann JD. Embodied cognition and the cerebellum: perspectives from the dysmetria of thought and the universal cerebellar transform theories. *Cortex*. 2018;100:140–8.
- Cabral J, Kringelbach ML, Deco G. Exploring the network dynamics underlying brain activity during rest. *Prog Neurobiol*. 2014;114:102–31.
- Habas C, Kamdar N, Nguyen D, Prater K, Beckmann CF, Menon V, et al. Distinct cerebellar contributions to intrinsic connectivity networks. *J Neurosci*. 2009;29(26):8586–94.
- Oakes TR, Fox AS, Johnstone T, Chung MK, Kalin N, Davidson RJ. Integrating VBM into the general linear model with voxelwise anatomical covariates. *Neuroimage*. 2007;34(2):500–8.
- Bagarinao E, Watanabe H, Maesawa S, Mori D, Hara K, Kawabata K, et al. An unbiased data-driven age-related structural brain parcellation for the identification of intrinsic brain volume changes over the adult lifespan. *Neuroimage*. 2018;169:134–44.
- Mioshi E, Dawson K, Mitchell J, Arnold R, Hodges JR. The Addenbrooke's cognitive examination revised (ACE-R): a brief cognitive test battery for dementia screening. *Int J Geriatr Psychiatry*. 2006;21(11):1078–85.
- Dos Santos Kawata KH, Hashimoto R, Nishio Y, et al. A validation study of the Japanese version of the Addenbrooke's cognitive examination-revised. *Dement Geriatr Cogn Dis Extra*. 2012;2(1):29–37.
- Wenning GK, Tison F, Seppi K, et al. Development and validation of the unified multiple system atrophy rating scale (UMSARS). *Mov Disord*. 2004;19(12):1391–402.
- Tsoi KK, Chan JY, Hirai HW, Wong SY, Kwok TC. Cognitive tests to detect dementia: a systematic review and meta-analysis. *JAMA Intern Med*. 2015;175(9):1450–8.
- Rittman T, Ghosh BC, McColgan P, Breen DP, Evans J, Williams-Gray CH, et al. The Addenbrook's cognitive examination for the differential diagnosis and longitudinal assessment of patients with parkinsonian disorders. *J Neurol Neurosurg Psychiatry*. 2013;84(5):544–51.
- Ashburner J. A fast diffeomorphic image registration algorithm. *Neuroimage*. 2007;38(1):95–113.
- Power JD, Barnes KA, Snyder AZ, Schlaggar BL, Petersen SE. Spurious but systematic correlations in functional connectivity MRI networks arise from subject motion. *Neuroimage*. 2012;59(3):2142–54.
- Beckmann CF, DeLuca M, Devlin JT, Smith SM. Investigations into resting-state connectivity using independent component analysis. *Philos Trans R Soc Lond Ser B Biol Sci*. 2005;360(1457):1001–13.
- Ray KL, McKay DR, Fox PM, et al. ICA model order selection of task co-activation networks. *Front Neurosci*. 2013;7:237.
- Filippini N, MacIntosh BJ, Hough MG, et al. Distinct patterns of brain activity in young carriers of the APOE-epsilon4 allele. *Proc Natl Acad Sci U S A*. 2009;106(17):7209–14.
- Mathotarachchi S, Wang S, Shin M, et al. VoxelStats: a MATLAB package for multi-modal voxel-wise brain image analysis. *Front Neuroinform*. 2016;10:20.

37. Xia M, Wang J, He Y. BrainNet viewer: a network visualization tool for human brain connectomics. *PLoS One*. 2013;8(7):e68910.
38. Smith SM, Fox PT, Miller KL, Glahn DC, Fox PM, Mackay CE, et al. Correspondence of the brain's functional architecture during activation and rest. *Proc Natl Acad Sci U S A*. 2009;106(31):13040–5.
39. Krienen FM, Buckner RL. Segregated fronto-cerebellar circuits revealed by intrinsic functional connectivity. *Cereb Cortex*. 2009;19(10):2485–97.
40. Buckner RL, Krienen FM, Castellanos A, Diaz JC, Yeo BT. The organization of the human cerebellum estimated by intrinsic functional connectivity. *J Neurophysiol*. 2011;106(5):2322–45.
41. Balsters JH, Laird AR, Fox PT, Eickhoff SB. Bridging the gap between functional and anatomical features of cortico-cerebellar circuits using meta-analytic connectivity modeling. *Hum Brain Mapp*. 2014;35(7):3152–69.
42. Lenka A, Bhalsing KS, Panda R, Jhunjhunwala K, Naduthota RM, Saini J, et al. Role of altered cerebello-thalamo-cortical network in the neurobiology of essential tremor. *Neuroradiology*. 2017;59:157–68.
43. Helmich RC, Hallett M, Deuschl G, Toni I, Bloem BR. Cerebral causes and consequences of parkinsonian resting tremor: a tale of two circuits? *Brain*. 2012;135:3206–26.
44. Filip P, Lungu OV, Bares M. Dystonia and the cerebellum: a new field of interest in movement disorders? *Clin Neurophysiol*. 2013;124:1269–76.
45. Filip P, Gallea C, Lehericy S, Bertasi E, Popa T, Marecek R, et al. Disruption in cerebellar and basal ganglia networks during a visuo-spatial task in cervical dystonia. *Mov Disord*. 2017;32:757–68.
46. Hubsch C, Roze E, Popa T, Russo M, Balachandran A, Pradeep S, et al. Defective cerebellar control of cortical plasticity in writer's cramp. *Brain*. 2013;136:2050–62.
47. Yao Q, Zhu D, Li F, Xiao C, Lin X, Huang Q, et al. Altered functional and causal connectivity of cerebello-cortical circuits between multiple system atrophy (parkinsonian type) and Parkinson's disease. *Front Aging Neurosci*. 2017;9:266.
48. Stoodley CJ, Schmahmann JD. Functional topography in the human cerebellum: a meta-analysis of neuroimaging studies. *Neuroimage*. 2009;44(2):489–501.
49. Euston DR, Gruber AJ, McNaughton BL. The role of medial prefrontal cortex in memory and decision making. *Neuron*. 2012;76(6):1057–70.
50. Yuan P, Raz N. Prefrontal cortex and executive functions in healthy adults: a meta-analysis of structural neuroimaging studies. *Neurosci Biobehav Rev*. 2014;42:180–92.
51. Salmi J, Pallesen KJ, Neuvonen T, Brattico E, Korvenoja A, Salonen O, et al. Cognitive and motor loops of the human cerebro-cerebellar system. *J Cogn Neurosci*. 2010;22(11):2663–76.
52. Stoodley CJ, Valera EM, Schmahmann JD. Functional topography of the cerebellum for motor and cognitive tasks: an fMRI study. *Neuroimage*. 2012;59(2):1560–70.
53. Habas C. Research note: a resting-state, cerebello-amygdaloid intrinsically connected network. *Cerebellum Ataxias*. 2018;5:4.
54. Benarroch EE. The amygdala: functional organization and involvement in neurologic disorders. *Neurology*. 2015;84(3):313–24.
55. Aminoff EM, Kveraga K, Bar M. The role of the parahippocampal cortex in cognition. *Trends Cogn Sci*. 2013;17(8):379–90.
56. Cykowski MD, Coon EA, Powell SZ, Jenkins SM, Benarroch EE, Low PA, et al. Expanding the spectrum of neuronal pathology in multiple system atrophy. *Brain*. 2015;138(Pt 8):2293–309.
57. Agosta F, Weiler M, Filippi M. Propagation of pathology through brain networks in neurodegenerative diseases: from molecules to clinical phenotypes. *CNS Neurosci Ther*. 2015;21(10):754–67.
58. Marien P, Manto M. Cerebellum as a master-piece for linguistic predictability. *Cerebellum*. 2018;17:101–3.
59. Bares M, Lungu O, Liu T, Waechter T, Gomez CM, Ashe J. Impaired predictive motor timing in patients with cerebellar disorders. *Exp Brain Res*. 2007;180:355–65.
60. Bares M, Lungu OV, Liu T, Waechter T, Gomez CM, Ashe J. The neural substrate of predictive motor timing in spinocerebellar ataxia. *Cerebellum*. 2011;10:233–44.
61. Husarova I, Mikl M, Lungu OV, Marecek R, Vanicek J, Bares M. Similar circuits but different connectivity patterns between the cerebellum, basal ganglia, and supplementary motor area in early Parkinson's disease patients and controls during predictive motor timing. *J Neuroimaging*. 2013;23:452–62.
62. Husarova I, Lungu OV, Marecek R, Mikl M, Gescheidt T, Krupa P, et al. Functional imaging of the cerebellum and basal ganglia during predictive motor timing in early Parkinson's disease. *J Neuroimaging*. 2014;24:45–53.
63. Sokolov AA, Miall RC, Ivry RB. The cerebellum: adaptive prediction for movement and cognition. *Trends Cogn Sci*. 2017;21:313–32.
64. Lawrenson C, Bares M, Kamondi A, Kovacs A, Lumb B, Apps R, et al. The mystery of the cerebellum: clues from experimental and clinical observations. *Cerebellum Ataxias*. 2018;5:8.
65. Franciotti R, Delli Pizzi S, Perfetti B, Tartaro A, Bonanni L, Thomas A, et al. Default mode network links to visual hallucinations: a comparison between Parkinson's disease and multiple system atrophy. *Mov Disord*. 2015;30(9):1237–47.
66. Watanabe H, Saito Y, Terao S, Ando T, Kachi T, Mukai E, et al. Progression and prognosis in multiple system atrophy: an analysis of 230 Japanese patients. *Brain*. 2002;125(Pt 5):1070–83.
67. Ozawa T, Revesz T, Paviour D, Lees AJ, Quinn N, Tada M, et al. Difference in MSA phenotype distribution between populations: genetics or environment? *J Park Dis*. 2012;2(1):7–18.
68. Damoiseaux JS, Prater KE, Miller BL, Greicius MD. Functional connectivity tracks clinical deterioration in Alzheimer's disease. *Neurobiol Aging*. 2012;33(4):828 e819–30.
69. Kalpouzos G, Persson J, Nyberg L. Local brain atrophy accounts for functional activity differences in normal aging. *Neurobiol Aging*. 2012;33(3):623 e621–13.

Publisher's Note Springer Nature remains neutral with regard to jurisdictional claims in published maps and institutional affiliations.